Model and simulation of a Vacuum Sieve Tray for T extraction from liquid PbLi breeding blankets

M. A. J. Mertens[a,1,*], D. Demange[b], L. Frances[b]

[a] Ghent University, Department of Materials Science and Engineering, Center of Molecular Modeling, Technologiepark 903, B-9052 Zwijnaarde, Belgium

[b] Karlsruhe Institute of Technology, Institute for Technical Physics, Tritium Laboratory Karlsruhe, Hermann-von-Helmholtz Platz 1, D-76344 Eggenstein-Leopoldshafen, Germany

Abstract

Tritium self-sufficiency within a nuclear fusion reactor is necessary to demonstrate nuclear fusion as a viable source of energy. Tritium can be produced within liquid eutectic PbLi but then has to be extracted to be refuelled to the plasma. The Vacuum Sieve Tray (VST) method is based on the extraction of tritium from millimetre-scaled oscillating PbLi droplets falling inside a vacuum chamber. A simulation tool was developed describing the fluid dynamics occurring along the PbLi flow and was used to study the influence of the different geometrical and operational parameters on the VST performance. The simulation predicts that extraction efficiencies over 90 % can be easily reached according to theory and previous experimental results. The size of the VST extraction unit for a fusion reactor is estimated based on the findings from our single-nozzle model and assuming no T reabsorption. It is found to be in the feasible range. Nevertheless, two approaches are discussed which may further reduce this size by up to 90 %. The simulation tool proved to be an easy and powerful way to analyse and optimise VST set-ups at any scale.

Keywords: Fusion, Breeding Blanket, Liquid PbLi, Tritium Extraction System, Vacuum Sieve Tray, Size Estimation

1. Introduction

In the perspective of D-T fusion, tritium self-sufficiency is a strong and challenging requirement for the design of a fusion reactor. A concept addressing this issue is the use of liquid eutectic lead-lithium (later in this text simply referred to as PbLi) in tritium breeding blankets surrounding the fusion plasma [1]. The neutrons produced in the fusion reactions can then interact with lithium to form tritium and helium. Lead, being a good neutron multiplier [2], corrects for the amount of neutrons being lost without interaction. The produced T has to be efficiently extracted from the liquid PbLi in order to fuel it into the plasma.

Previously proposed methods to do this e.g. Gas Liquid Contactors [3], Permeator Against Vacuum [4], Regenerable Getters [5] are still being evaluated but do not yet match the DEMO requirements. An old method, the Vacuum Sieve Tray (VST), is regaining interest because of newly discovered highlights [6]. This method is based on the passive extraction of T from millimetre-scale PbLi droplets falling in a vacuum tank. It was wrongly rejected before because the T transport within the droplet was thought to be diffusion-governed and therefore too slow [7]. Recent VST experiments with deuterium at the Kyoto University [6, 8, 9, 10] however showed that the droplets oscillate after detaching from the injected PbLi jet. The authors suggested that these oscillations result in internal fluid element circulation and promote the transport of T, which is then no longer diffusion governed, towards the surface. This phenomenon can explain the significant boost measured in extraction rate and makes the VST method very promising.

We developed a simulation tool describing the fluid dynamics occurring along the PbLi flow in a virtual experiment. This model helps to get a better insight in the characteristics inherent to the VST method, allows designing a unique and efficient experimental VST device and can be used to upscale the method to relevant breeding blanket characteristics .

2. Simulated VST set-up

The simulation is based on the set-up used at the Kyoto University and is shown in Figure 1. In this configuration, the upper tank is used to dissolve deuterium in the liquid PbLi (mimicking the conditions of T bred within PbLi by an external neutron source). This upper tank is connected to a lower tank maintained under dynamic vacuum. The connection ends in a sub-millimetre nozzle at the top of the lower tank and can be opened or closed using a valve V. After the PbLi is saturated with deuterium, the actual

*Corresponding author: merlijn.mertens@ugent.be

[1] PhD Fellowship of the Research Foundation - Flanders (FWO)

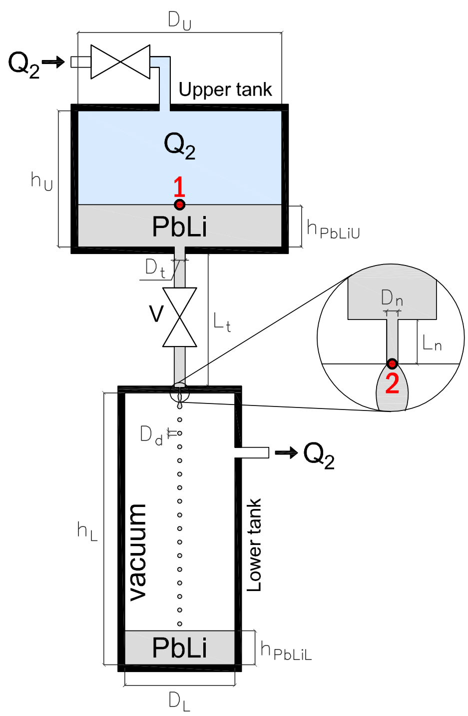

Figure 1: Schematic view of the simulated set-up. Here D=diameter, h=height, L=length, V=valve, Q_2=hydrogen isotope gas while the indices U, L, t, n and d are used to denote properties of respectively the upper tank, the lower tank, the connection tube, the nozzle and the PbLi droplets. Also the two points used in the Bernoulli equation (Eq.3) are indicated.

extraction experiment is started by opening valve V resulting in a fine jet of liquid PbLi being injected in the lower tank. The unstable PbLi jet almost instantaneously breaks up in separate oscillating millimetre-sized droplets from which deuterium is extracted and collected by the vacuum pumps. The main aim of the developed simulation tool is to calculate the extraction efficiency of deuterium/tritium from PbLi for given operational conditions and dimensions of the device (i.e. tanks, connection tube, nozzle) and to examine how this quantity varies along the experiment.

3. Mathematical model

The tritium extraction efficiency is defined as the ratio of the amount of tritium extracted to the amount of tritium initially dissolved in the PbLi. This extraction efficiency has been studied for deuterium in the Kyoto University and Eq.(1) was proposed to describe this process [6, 11]:

$$\eta(t) = 1 - \frac{6}{\pi^2}\sum_{n=1}^{\infty}\frac{1}{n^2}\exp\left(\frac{-D\cdot n^2\cdot\pi^2\cdot t_f(t)}{\left(\frac{D_d}{2}\right)^2}\right) \tag{1}$$

In this equation $\eta(t)$ is the time-dependent extraction efficiency, t_f is the falling time of the droplet varying along the experiment, D_d is the droplet diameter and D is a coefficient describing the transport of deuterium from within the droplet towards its surface. If this transport would be diffusion-governed, as initially thought, this coefficient would be the diffusion coefficient. However the deuterium transport was found to be considerably enhanced by the oscillation of the droplets, therefore a quasi dispersion coefficient D was defined and fitted to the experimentally measured amounts of extracted deuterium. This led to a value of $D = 3.4\times10^{-7}\,\mathrm{m^2/s}$ [6] which is about 300 times bigger than the diffusion coefficient reported by Reiter et al. [12]. It must be noted that this value can only be safely used within the range of the geometrical and operational parameters in which it was obtained (e.g. nozzle diameters between 0.4 and 1 mm). From the Plateau-Rayleigh instability analysis for a fluid jet, it can be derived that the droplet diameter D_d is directly proportional to the nozzle diameter and is described by $D_d = 1.89\,D_n$. This was also experimentally validated for nozzle diameters ranging between 0.4 and 1 mm [9].

The falling time of the droplet t_f depends on two quantities: (i) the velocity v_n at which the PbLi exits the nozzle at the top of the upper tank and (ii) the falling height of the droplet h_f. Both of these quantities vary with time for the described set-up (but not when implemented in a fusion reactor). Indeed, during the experiment PbLi accumulates in the lower tank and therefore the height of the PbLi level in the lower tank h_{PbLiL} increases. As a result the falling height h_f reduces. The time dependence of the falling time t_f can then be described by Eq.(2):

$$t_f(t) = \frac{-v_n(t) + \sqrt{v_n^2(t) + 2\,g\,(h_L - h_{PbLiL}(t))}}{g} \tag{2}$$

In this equation g is the gravitational acceleration and h_L is the total height of the lower tank.

In order to calculate the nozzle exit velocity v_n, the extended Bernoulli equation, which is based on the conservation of energy within the system, is used . All terms in this equation are commonly expressed in terms of heads (units m). The total energy is compared at two points: (1) at the surface of the PbLi in contact with the tritium gas and (2) at the outlet of the nozzle (as depicted on Figure 1). The extended Bernoulli equation (Eq.3) states:

$$\frac{v_1^2}{2g} + \frac{p_1}{\rho g} + h_1 = \frac{v_2^2}{2g} + \frac{p_2}{\rho g} + h_2 + h_{L_{1\to2}} \tag{3}$$

In this equation the first term accounts for the kinetic energy with v_i the mean velocity of the fluid at point i. The second term results from the potential energy due to the ambient pressure p_i with ρ the density of the PbLi. The third term corresponds to the potential energy due to the hydrostatic pressure with h_i the height of the fluid at point i. The term $h_{L_{1\to2}}$ accounts for all friction losses. Two assumptions were made here: (i) the temperature of the PbLi is the same at the two considered points so that no heat losses are considered, (ii) all possible convection effects are neglected and (iii) the PbLi is considered to be an incompressible fluid so that the density remains constant.

Some simplifications can be made at this point. As the lower tank is maintained under vacuum, the ambient pressure at the second point is negligible compared to the one at the first point, therefore $p_2 = 0$ is assumed. Additionally, the origin of the height-scale can be chosen in the second point so that $h_2 = 0$. Finally, as the diameter of the upper tank is of the order of tens of centimetres while the nozzle diameters are of the order of (sub-)millimetre and because of mass conservation (for an incompressible flow this means $v_1 A_1 = v_2 A_2$ with A the surface cross section), the velocity at the first point will be negligibly small compared with the ones occurring at the outlet of the nozzle and $v_1 = 0$ can be assumed. The discussion above allows to rewrite Eq.(3) as follows:

$$\frac{p_{\mathrm{T}_2}}{\rho g} + h_{\mathrm{PbLi}} = \frac{v_{\mathrm{n}}^2}{2g} + h_{\mathrm{L}_{1\to 2}} \tag{4}$$

where h_{PbLi} is the height of the PbLi surface with respect to the outlet of the nozzle and p_{T_2} the pressure of the tritium gas in the upper tank.

Five contributions to the total head loss due to friction and geometry changes were identified:

- the contraction at the connection tube inlet $h_{\mathrm{L}_{(\mathrm{UT}\to\mathrm{t})}}$,
- the viscous losses in the connection tube $h_{\mathrm{L}_{(\mathrm{t})}}$,
- the head loss in the valve $h_{\mathrm{L}_{(\mathrm{V})}}$,
- the contraction at the nozzle inlet $h_{\mathrm{L}_{(\mathrm{t}\to\mathrm{n})}}$,
- the viscous losses in the nozzle $h_{\mathrm{L}_{(\mathrm{n})}}$.

The total head loss between points 1 and 2 is then the sum of all these contributions:

$$h_{\mathrm{L}_{1\to 2}} = h_{\mathrm{L}_{(\mathrm{UT}\to\mathrm{t})}} + h_{\mathrm{L}_{(\mathrm{t})}} + h_{\mathrm{L}_{(\mathrm{V})}} + h_{\mathrm{L}_{(\mathrm{t}\to\mathrm{n})}} + h_{\mathrm{L}_{(\mathrm{n})}} \tag{5}$$

Each contribution was calculated from the theory of fluid dynamics and can be expressed as a function of the total volumetric flow rate Q, which is constant throughout the piping system - tube, valve and nozzle - as a result of the incompressibility of liquid PbLi ($Q = v_{\mathrm{n}} A_{\mathrm{n}} = v_{\mathrm{t}} A_{\mathrm{t}}$):

$$h_{\mathrm{L}_{(\mathrm{UT}\to\mathrm{t})}} = 0.5 \frac{Q^2}{2gA_{\mathrm{t}}^2} \tag{6}$$

$$h_{\mathrm{L}_{(\mathrm{t})}} = f_{\mathrm{t}}(Q) \frac{L_{\mathrm{t}}}{D_{\mathrm{t}}} \frac{Q^2}{2gA_{\mathrm{t}}^2} \tag{7}$$

$$h_{\mathrm{L}_{(\mathrm{V})}} = K_{\mathrm{L}_{(\mathrm{V})}} \frac{Q^2}{2gA_{\mathrm{t}}^2} \tag{8}$$

$$h_{\mathrm{L}_{(\mathrm{t}\to\mathrm{n})}} = 0.5 \left(1 - \left(\frac{D_n}{D_t}\right)^2\right)^2 \frac{Q^2}{2gA_{\mathrm{n}}^2} \tag{9}$$

$$h_{\mathrm{L}_{(\mathrm{n})}} = f_{\mathrm{n}}(Q) \frac{L_{\mathrm{n}}}{D_{\mathrm{n}}} \frac{Q^2}{2gA_{\mathrm{n}}^2} \tag{10}$$

In the equations above, the indices t and n refer to the tube and nozzle. The velocities are denoted by v_{x} ($\mathrm{x} = \mathrm{t}, \mathrm{n}$), the cross section areas by A_{x}, the diameters by D_{x}, the lengths by L_{x} and the volume flow rate by Q. $K_{\mathrm{L(V)}}$ is the loss coefficient of the valve which depends on the type of valve. The f_{x} is the Darcy friction factor which has a different mathematical description for laminar and turbulent flow regimes. For laminar flows in circular pipes ($Re < 2300$), it is given by:

$$f_{\mathrm{x}} = \frac{64}{Re_{\mathrm{x}}} \tag{11}$$

For turbulent flows in circular pipes ($Re > 4000$), it is described by the Colebrook-White equation [13]:

$$\frac{1}{\sqrt{f_{\mathrm{x}}}} = -2.0 \cdot \log_{10}\left(\frac{1}{3.7}\frac{e_{\mathrm{x}}}{D_{\mathrm{x}}} + \frac{2.51}{Re_{\mathrm{x}}\sqrt{f_{\mathrm{x}}}}\right) \tag{12}$$

Here e_{x} is the absolute roughness of the pipe (tube/nozzle) and Re_{x} is the Reynolds number given by:

$$Re_{\mathrm{x}} = \frac{v_{\mathrm{x}} D_{\mathrm{x}}}{\nu} = \frac{\rho v_{\mathrm{x}} D_{\mathrm{x}}}{\mu} \tag{13}$$

with ν the kinematic viscosity and μ the dynamic viscosity.

In the first simulations, it was assumed to have turbulent flows in both the tube and in the nozzle. This was checked and the flow in the nozzle was found to be always turbulent. The flow regime in the tube could vary from laminar to turbulent. It will however be shown in section 5 of this article that the flow regime in the tube is insignificant for our flow calculations. Eq.(12) is a non-linear equation which has to be solved by iteration. To save computing time, an alternative explicit approximation, the Serghides equation, was used which offers high precision ($< 0.003\,\%$) in the ranges $4000 < \mathrm{Re} < 10^{10}$ and $10^{-7} <$ relative roughness < 1 [14, 15]. This equation reduces the computing time by a factor 10 and is given by:

$$f_{\mathrm{x}} = \left(A_{\mathrm{x}} - \frac{(B_{\mathrm{x}} - A_{\mathrm{x}})^2}{C_{\mathrm{x}} - 2B_{\mathrm{x}} + A_{\mathrm{x}}}\right)^{-2} \tag{14}$$

with

$$A_{\mathrm{x}} = -2\log_{10}\left(\frac{1}{3.7}\frac{e_{\mathrm{x}}}{D_{\mathrm{x}}} + \frac{12}{Re_{\mathrm{x}}}\right) \tag{14a}$$

$$B_{\mathrm{x}} = -2\log_{10}\left(\frac{1}{3.7}\frac{e_{\mathrm{x}}}{D_{\mathrm{x}}} + \frac{2.51A}{Re_{\mathrm{x}}}\right) \tag{14b}$$

$$C_{\mathrm{x}} = -2\log_{10}\left(\frac{1}{3.7}\frac{e_{\mathrm{x}}}{D_{\mathrm{x}}} + \frac{2.51B_{\mathrm{x}}}{Re_{\mathrm{x}}}\right) \tag{14c}$$

The expressions for the different pressure losses can be introduced in Eq.(4) which can be rewritten as:

$$\begin{aligned} &\frac{p_{\mathrm{T}_2}}{\rho g} + h_{\mathrm{PbLi}} - \frac{Q^2}{2gA_{\mathrm{n}}^2} - \frac{0.5\,Q^2}{2gA_{\mathrm{t}}^2} - f_{\mathrm{t}}(Q)\frac{L_{\mathrm{t}}}{D_{\mathrm{t}}}\frac{Q^2}{2gA_{\mathrm{t}}^2} - \frac{K_{\mathrm{L(V)}}Q^2}{2gA_{\mathrm{t}}^2} \\ &- 0.5\left(1 - \left(\frac{D_n}{D_t}\right)^2\right)^2 \frac{Q^2}{2gA_{\mathrm{n}}^2} - f_{\mathrm{n}}(Q)\frac{L_{\mathrm{n}}}{D_{\mathrm{n}}}\frac{Q^2}{2gA_{\mathrm{n}}^2} = 0 \end{aligned} \tag{15}$$

This is a non-linear equation which is solved by iteration. The result is a value for Q which allows calculating the velocity of the PbLi at the exit of the nozzle:

$$v_{\mathrm{n}} = \frac{Q}{A_{\mathrm{n}}} = \frac{4Q}{\pi D_{\mathrm{n}}^2} \tag{16}$$

This result is used to calculate the droplet falling time $t_{\mathrm{f}}(\mathrm{t})$ and the extraction efficiency $\eta(\mathrm{t})$ using respectively Eq.(2) and Eq.(1).

4. Simulation code

The input data of the simulation can be separated in two distinct groups (as listed in Table 1). The first group of input parameters describes the geometry of the device i.e the dimensions, shape and absolute roughness of both tanks, the tube and the nozzle. The second group describes the chosen operative conditions i.e. the equilibrium pressure of the tritium gas in the upper tank after the dissolution process, the temperature T of the system (the liquid PbLi and tritium gas are assumed to be in thermal equilibrium) and the initial amount of PbLi in the upper tank. These conditions are then used to calculate the relevant physical properties of the PbLi and the tritium gas:

$$\rho_{\mathrm{PbLi}} = 10520.42 - (1.19064\,T) \tag{17}$$

$$\mu_{\mathrm{PbLi}} = 0.187 \times 10^{-3} \exp\left(\frac{1400}{T}\right) \tag{18}$$

$$p_{\mathrm{vap}}^{\mathrm{PbLi}} = 1.5 \times 10^{10} \exp\left(-\frac{22900}{T}\right) \tag{19}$$

$$K_{\mathrm{S}} = 2.32 \times 10^{-8} \exp\left(-\frac{1350}{RT}\right) \tag{20}$$

Here ρ_{PbLi} is the density of PbLi [16], μ_{PbLi} the dynamic viscosity of PbLi [16], $p_{\mathrm{vap}}^{\mathrm{PbLi}}$ the vapour pressure of PbLi [17] and K_{S} the Sieverts constant of $\mathrm{T_2}$ in PbLi according to Reiter et al. [12]. The density and dynamic viscosity are required to describe the fluid dynamics of PbLi within the system. The vapour pressure has no effect on the follow up of the experiment but was nevertheless calculated as it sets a lower limit to the allowed vacuum pressure in the lower tank to avoid the boiling of PbLi. The Sieverts constant indicates the amount of tritium gas dissolved in the PbLi for a given equilibrium pressure:

$$x_{\mathrm{T}} = K_{\mathrm{S}} \sqrt{p_{\mathrm{T_2}}^{\mathrm{eq}}} \tag{21}$$

Here, x_{T} is the atomic fraction of tritium dissolved in PbLi, K_{S} is the Sieverts constant expressed in atomic fraction$\cdot\mathrm{Pa}^{-0.5}$ and $p_{\mathrm{T_2}}^{\mathrm{eq}}$ is the equilibrium pressure of $\mathrm{T_2}$. It should be remarked that huge discrepancies exist on the reported values for the Sieverts constant (about two orders of magnitude [12, 18, 19, 20, 21]). When working on safety issues and inventory calculation of T in the system a high Sieverts constant should be used, while for detectability issues of extracted tritium a small Sieverts constant should be used. When studying the extraction efficiency, any value can be used because it does not influence the relative amount of tritium being extracted.

The size of the time step was automatically adapted to the initial mass flow rate to have a similar amount of time steps in all simulations. The simulation finally provides a complete follow up of the experiment i.e. the time evolution of the nozzle exit velocity $v_{\mathrm{n}}(t)$, the mass flow rate $Q_{\mathrm{M}}(t)$, the height of the PbLi surface in the upper tank $h_{\mathrm{PbLiU}}(t)$ and in the lower tank $h_{\mathrm{PbLiL}}(t)$, the extraction efficiency $\eta(t)$, etc. Additionally it returns output values specific for one entire experiment such as the experiment's total duration t_{exp} and the global extraction efficiency Eff_{g}. The duration follows directly from the simulation. The global efficiency is calculated using the following equation:

$$Eff_{\mathrm{g}} = \frac{\int_{\mathrm{start}}^{\mathrm{end}} \eta(t)\, Q_V(t)\, \mathrm{d}t}{\int_{\mathrm{start}}^{\mathrm{end}} Q_V(t)\, \mathrm{d}t} \approx \frac{\sum_{i=1}^{\mathrm{end}} (\eta_i + \eta_{i+1})\, \Delta V_{i\to i+1}}{2V_{\mathrm{PbLi}}} \tag{22}$$

In this equation, Eff_{g} is the global efficiency of the experiment, $\eta(t)$ is the extraction efficiency at time t, $Q_V(t)$ is the volume flow rate at time t, V_{PbLi} is the total volume of the PbLi used in the experiment, η_i is the efficiency at time t_i and $\Delta V_{i\to i+1}$ is the volume of PbLi flowing through the nozzle between time t_i and time t_{i+1}. In this equation every efficiency value is thus weighted by the PbLi volume it accounts for.

5. Results for a case study

In this case study, a realistic input parameter set was used to investigate the typical characteristics of a VST experiment. The input is shown in Table 1. Here, the same valves as in the experiments with deuterium are considered i.e. Swagelok bellow-sealed valves of type V51, which have a flow coefficient C_v of $0.36\,\mathrm{gpm}/\sqrt{\mathrm{psi}}$ [22]. This flow coefficient can be converted in the loss coefficient $K_{\mathrm{L(V)}}$ using [23]:

$$K_{\mathrm{L(V)}} = \frac{891 d^4}{C_v^2} \tag{23}$$

where the inner diameter of the tube d is expressed in inches. The tube in this case study has an inner diameter of 4.6 mm (0.1811 inch). This results in a loss coefficient of about 7.4.

To deepen the understanding of the different head loss contributions, they were plotted together with the other terms from Eq.(15) for a simulation with a 0.6 mm nozzle diameter (Figure 2). In this plot $\mathrm{v_{diff}}$ represents the kinetic energy term, $\mathrm{p_{diff}}$ is the ambient pressure term, $\mathrm{h_{diff}}$ is the hydrostatic pressure term and the remaining curves

Geometry			
Name	Symbol	Value	Unit
Nozzle length	L_{n}	2	mm
Nozzle diameter	D_{n}	0.4 - 1	mm
Nozzle absolute roughness	e_{n}	1	µm
Tube length	L_{t}	27.5	cm
Tube inner diameter	D_{t}	4.6	mm
Tube absolute roughness	e_{t}	1	µm
Valve loss coefficient	$K_{\mathrm{L(V)}}$	7.4	-
Volume upper tank	V_{U}	4	l
Height/diameter upper tank	$R_{h/D}$	0.3	-
Height lower tank	h_{L}	1	m
Diameter lower tank	D_{L}	0.3	m
Conditions			
PbLi amount	m_{PbLi}	10	kg
Equilibrium T_2 pressure	p_{eq}	40000	Pa
PbLi temperature	T	400	°C

Table 1: Input parameters used in the case study.

represent the five contributions to the total head loss between the two considered points (see Figure 1). Eq. (15) can be rewritten as:

$$p_{\mathrm{diff}}+h_{\mathrm{diff}}-v_{\mathrm{diff}}-h_{\mathrm{L_{(UT\to t)}}}-h_{\mathrm{L_{(t)}}}-h_{\mathrm{L_{(V)}}}-h_{\mathrm{L_{(t\to n)}}}-h_{\mathrm{L_{(n)}}}=0 \tag{24}$$

The largest terms in Eq.(24) proved to be the terms resulting from the velocity, height and pressure difference between the 2 considered points. However also relative large contributions result from the head loss in the tube-to-nozzle transition and the frictional losses in the nozzle. The head loss in the valve, the tube and at the transition from the upper tank to tube are negligible compared to the other terms. This was found to be always the case even for a laminar flow regime in the tube (using Eq.(11) instead of Eq.(14) for the Darcy friction factor) and these terms can thus be omitted in Eq.(15). Therefore the flow regime occurring in the tube is not of importance.

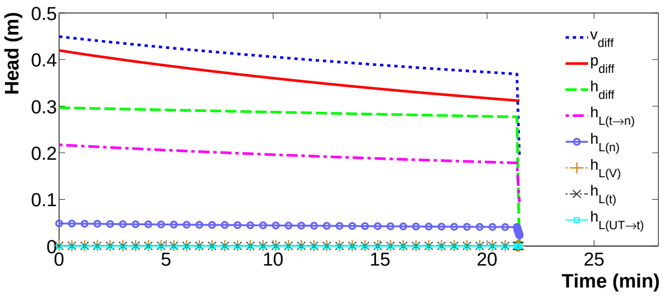

Figure 2: The importance of the terms in the extended Bernoulli equation (input parameters: see Table 1 and D_{n} = 0.6 mm).

Figure 3 shows the total PbLi mass flow rate for different nozzle diameters as a function of time. As expected the mass flow is lower for smaller nozzle diameters. This is because of (i) the smaller cross section area through which the fluid can flow ($Q_{\mathrm{M}} = v_{\mathrm{n}}A_{\mathrm{n}}\rho_{\mathrm{PbLi}}$) and (ii) a smaller nozzle induces higher head losses in the nozzle (Eq.10) and at the tube-to-nozzle transition (Eq.9) which results in a decreased nozzle exit velocity. As the PbLi leaves the upper tank during the experiment, more volume becomes available for the tritium gas and therefore its pressure drops. Additionally, the hydrostatic pressure of the PbLi at the exit of the nozzle decreases because of the dropping PbLi level. The two forces driving the PbLi flow are thus both decreasing during the experiment which explains the falling mass flow rates in Figure 3. The final fast drop occurs when the PbLi level reaches the connection tube with a considerably smaller diameter than the upper tank. The PbLi level then quickly drops and therefore also the hydrostatic pressure at the nozzle exit.

When all PbLi has left the upper tank, the simulation stops. It can immediately be seen that a complete experiment with a nozzle of 1 mm is considerably shorter than one with a nozzle of 0.4 mm (8 min vs. 50 min for the given set of input parameters). The integrals of all four curves are the same and equal to the initial amount of PbLi in the upper tank (here 10 kg).

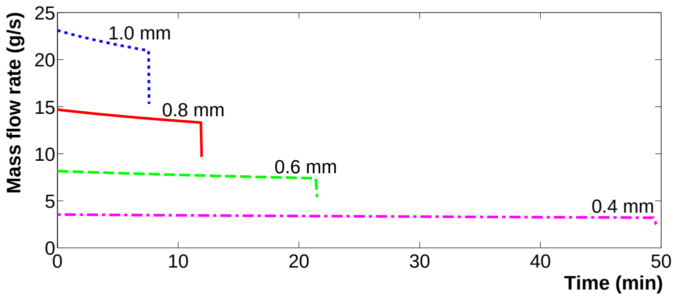

Figure 3: The time evolution of the PbLi mass flow rate for different nozzle diameters (input parameters: see Table 1).

Figure 4 shows the time dependence of the extraction efficiency for the same conditions. It can be seen that the extraction efficiency is higher for smaller nozzle diameters. This is mainly because smaller droplets results in higher extraction efficiencies according to Eq.(1) ($D_{\mathrm{d}} = 1.89D_{\mathrm{n}}$). Additionally, the lower exit velocities for small nozzle diameters (initially 2.89 m/s for the 0.4 mm nozzle compared to 3.03 m/s for the 1 mm nozzle) result in a longer falling time (0.245 s versus 0.238 s) and therefore a higher extraction efficiency (see Eq.1). Two different effects influence the time variation of extraction efficiency: (i) the decreasing nozzle exit velocity which tends to increase the efficiency (ii) the decreasing falling height due to the accumulation of PbLi in the lower tank which tends to decrease the extraction efficiency. From the increasing tendency of the curves in Figure 4 we conclude that the first effect is dominant for the used input parameters. It is noted that the calculated extraction efficiency is quite high for all nozzle diameters considered (initially 0.998, 0.951, 0.850 and 0.747 for nozzle diameters of 0.4 mm, 0.6 mm, 0.8 mm and 1 mm respectively).

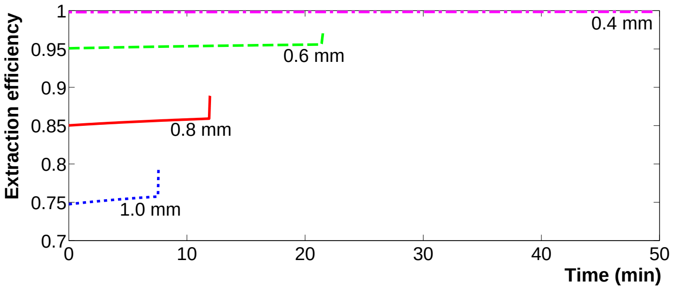

Figure 4: The time evolution of the extraction efficiency for different nozzle diameters (input parameters: see Table 1).

It is clear that a high efficiency can always be achieved at the cost of a long experiment's duration or equivalently a small mean mass flow rate. Therefore, the efficiency and mass flow must be considered together. It was investigated how the use of different nozzle diameters simultaneously influences the mean mass flow and the global extraction efficiency. The result is shown in Figure 5.

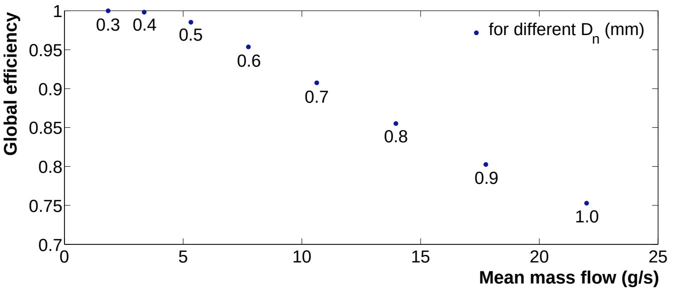

Figure 5: The global extraction efficiency and Pbli mean mass flow rate for different nozzle diameters (input parameters: see Table 1).

The trade-off between mass flow and efficiency is indeed found. The combination of both a high efficiency and large mass flow is desired as in a later stage the technique will have to be upscaled to match the high mass flows occurring in breeding blankets (current estimations are 560 kg/s in the HCLL and WCLL breeding blanket concepts and 46000 kg/s in DCLL [24, 25]). For nozzle diameters between 0.5 mm and 1 mm the efficiency decreases almost linearly with increasing mass flow rate. For nozzle diameters smaller than 0.5 mm, the efficiency grows very close to 1 while the mean mass flow still decreases considerably (for the conditions depicted in Table 1). Therefore the use of extremely small nozzle diameters proves to be disadvantageous when a high efficiency and large mass flow is desired simultaneously.

6. Upscaling VST to a Tritium Extraction System

To process the large PbLi mass flow rates occurring in actual breeding blankets, multiple nozzles will have to be

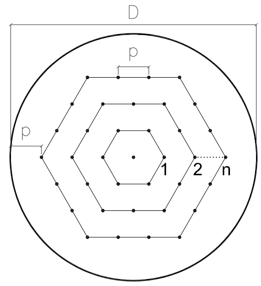

Figure 6: The proposed hexagonal nozzle configuration consisting out of one central nozzle and n hexagons surrounding it. The pitch p is the distance between two neighbouring nozzles and is also chosen to be the distance between the outermost nozzles and the wall of the tank. The resulting diameter D of the vacuum tank is also denoted.

D_n (mm)	h_{VT} (m)	N_n ($\times 10^4$)	D_{VT} (m)	V_{VT} (m^3)	η -
HCLL/WCLL (560 kg/s)					
0.4	1.0	16.7	4.74	17.6	0.998
1.0	1.0	2.55	1.86	2.72	0.754
1.0	10	2.55	1.86	27.2	0.992
DCLL (46 000 kg/s)					
0.4	1.0	1370	42.8	1439	0.998
1.0	1.0	210	16.7	220	0.754
1.0	10	210	16.7	2200	0.992

Table 2: Estimate of the number of nozzles N_n, the required diameter of the vacuum tank D_{VT}, the volume of the vacuum tank V_{VT} and the extraction efficiency η for different nozzle diameters D_n and vacuum tank heights h_{VT} for both HCLL/WCLL en DCLL breeding blankets

implemented. This is because a significant increase in nozzle diameter to increase the mass flow rate would plunge the extraction efficiency. Different nozzle configurations are possible and in the elaboration below a hexagonal one is considered (Figure 6), as it can be easily fitted on top of a cylindrical tank and it is easy to upscale using only one parameter i.e. the pitch p (the distance between neighbouring nozzles). This approach has also been used before e.g. by Longhurst and Dolan [26]. The pitch is chosen to be 1 cm which is assumed to be a conservative value to avoid coalescence and to limit the effects of reabsorption of extracted T by neighbouring droplets [27]. The mean mass flow rates per nozzle used in this section were all deduced from the single-nozzle simulation code. In the following first size estimate, the same conditions were assumed as in the case study discussed above (except for the lower tank's dimensions). For this simple model, the number of nozzles required to match the mass flow rates occurring in (i) HCLL/WCLL and (ii) DCLL breeding blankets was calculated. This number of nozzles could then be directly translated in a diameter for the cylindrically shaped vacuum tank considering the hexagonal nozzle configuration in Figure 6. The result is shown in Table 2.

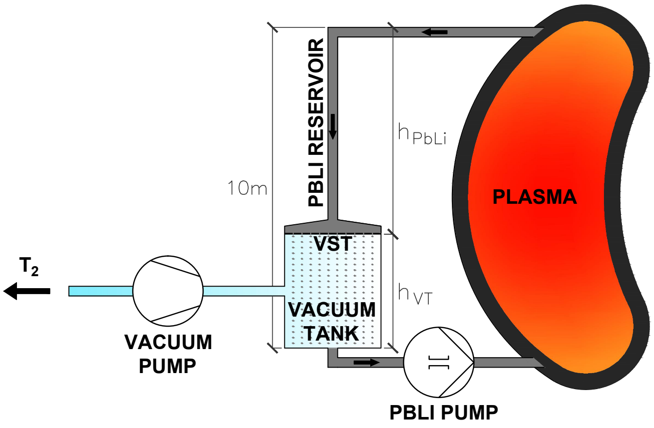

Figure 7: The considered VST implementation in the second method to reduce the vacuum tank size. The height of the vacuum vessel containing the plasma is comparable to the one designed for ITER [28].

It can be seen that the predicted diameters are especially realistic for the HCLL and WCLL concepts. But also for the high PbLi mass flow rates in a DCLL blanket, the estimated size is feasible. By increasing the height of the vacuum tank up to a realistic value of 10 m, high efficiencies can be reached even for nozzles with a diameter of 1 mm. This makes the VST method a viable and promising tritium extraction system candidate.

The achieved efficiency of 0.992 for this configuration is far above the minimal required efficiency of 0.8 in DEMO. Therefore, although already feasible in size, the extraction system can be made even more compact whilst keeping the efficiency higher than 0.8 by increasing the mass flow rate per nozzle. This can be achieved in 2 ways: (i) by increasing the diameter of the nozzles or (ii) by increasing the hydrostatic pressure at the nozzle's outlet making use of a PbLi reservoir on top of the nozzle tray (Figure 7).

In the first method the same reasoning is used as before. The additional assumption here is that all extraction phenomena can be upscaled to nozzle diameters higher than 1 mm. The droplet formation and behaviour beyond a 1.0 mm nozzle diameter have to be experimentally checked. As a first approach, the equation $D_\mathrm{d} = 1.89\,D_\mathrm{n}$ was simply extrapolated in the simulation. Following this reasoning, the largest nozzle diameter resulting in an extraction efficiency higher than 0.8 for a vacuum tank height of 10 m is found to be 1.9 mm (efficiency = 0.82). This configuration ultimately results in vacuum tank diameters of $D_\mathrm{HCLL/WCLL} = 1.0\,\mathrm{m}$ and $D_\mathrm{DCLL} = 8.98\,\mathrm{m}$.

A second alternative method consists in adding a PbLi reservoir on top of the VST. The simulation code was appropriately adapted to model the VST implementation imaged in Figure 7. Here it is assumed that the pumping power is not higher than what is required to pump the liquid PbLi through the blanket to the top of the device. The VST extraction system then operates purely passively under the influence of gravity (the hydrostatic pressure is the only driving force). The total height of the tritium extraction system was set to 10 m, which is considered to be a conservative value, even regarding the dimensions of ITER [28]. It can be subdivided over two different contributions: (i) the height of PbLi reservoir h_PbLi above the nozzle array which will define the hydrostatic pressure at the nozzle outlets and (ii) the height of the vacuum tank h_VT. The simulations were performed varying the ratio of these contributions and the result is shown in Figure 8.

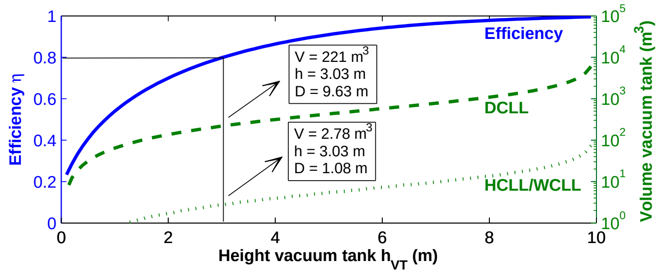

Figure 8: The extraction efficiency and the volume of the vacuum tank as a function of the height of the vacuum tank resulting from the configuration imaged in Figure 7 for the HCLL, WCLL and DCLL blanket concepts.

When the height of the PbLi reservoir is increased (and thus the height of the vacuum tank is decreased), the hydrostatic pressure at the nozzle outlets will increase and therefore the mass flow rate per nozzle. This will however also reduce the efficiency. The higher mass flow rate per nozzle reduces the amount of nozzles necessary to process a given total mass flow rate which results in a smaller required diameter of the vacuum tank. In this approach it is assumed that the mathematical model used so far to calculate the droplet's diameter, velocity and oscillation behaviour (and thus the extraction efficiency) is still valid, despite the higher mass flow rates resulting from the increased hydrostatic pressure. If an efficiency of 0.8 is demanded, this procedure can be used to reduce the VST diameter from 1.86 m to 1.08 m for HCLL/WCLL and from 16.7 m to 9.63 m for DCLL. This is only slightly higher than what was achieved by increasing the nozzle diameter to 1.9 mm. However, as the height of the vacuum tank is also diminished here, the vacuum tank volume is reduced considerably more ($2.78\,\mathrm{m}^3$ instead of $7.85\,\mathrm{m}^3$ for HCLL/WCLL and $221\,\mathrm{m}^3$ instead of $633\,\mathrm{m}^3$ for DCLL). This vacuum tank volume reduction of 90 % compared to the first size estimate will have a large impact on the required power of the vacuum pumps and therefore on the cost.

It is concluded that adding a PbLi reservoir is more desirable than increasing the nozzle diameters as the former results in considerably smaller vacuum tank volumes and more assumptions are associated with the latter. In order to validate these assumptions, dedicated experiments studying T reabsorption in neighbouring droplets and large nozzle diameter effects should be performed.

7. Conclusion

The simulation, describing the fluid dynamics occurring along the PbLi flow in a VST experiment, allows to gain a better insight in how the geometry of the VST set-up and the experimental conditions can influence the results. These insights can be used to optimise the experimental device before it is being build to effectively proof the working principle of VST for the extraction of tritium from liquid PbLi. It was found that high extraction efficiencies can be expected when using the VST method which would be a breakthrough in the field of Tritium Extraction Systems in breeding blankets. A compromise will have to be made between the mean mass flow rate and the desired extraction efficiency as the TES will have to process the large PbLi mass flows occurring in actual breeding blankets. The size of the VST extraction units for both HCLL/WCLL and DCLL breeding blankets for DEMO was estimated based on the results from the single-nozzle model and assuming no T reabsorption. Both were found to be in a realistic and feasible range. Making additional assumptions, two approaches were proposed which may further reduce the size of the VST extraction unit. The most promising one makes use of a PbLi reservoir above the nozzle array which allows to considerably increase the mass flow rate per nozzle. Assuming that the oscillating behaviour of the droplets in not influenced by this increased mass flow, one can achieve a significant reduction of the size of the required vacuum tank (90 % volume reduction compared to the first estimate).

To demonstrate the relevance of the VST method to extract tritium from liquid PbLi and to validate the simulation tool, an experimental set-up is currently being designed and should be operated with T at the Tritium Laboratory of Karlsruhe (TLK). Additionally, a multi-nozzle experiment and a large nozzle diameter experiment are required to improve the reliability of the VST extraction unit size estimates.

8. Acknowledgements

This research project was completed as Master thesis for the Erasmus Mundus European Master in Nuclear Fusion and Engineering Physics. The article was written during a PhD Fellowship of the Research Foundation - Flanders (FWO). The work has been carried out within the framework of the EUROfusion Consortium and has received funding from the European Union's Horizon 2020 research and innovation programme under grant agreement number 633053. The views and opinions expressed herein do not necessarily reflect those of the European Commission.

9. References

[1] M. Abdou, N. B. Morley, S. Smolentsev, A. Ying, S. Malang, A. Rowcliffe, M. Ulrickson, Blanket/first wall challenges and required R&D on the pathway to DEMO, Fusion Engineering and Design 100 (2015) 2–43. doi:10.1016/j.fusengdes.2015.07.021.

[2] V. Ashby, H. Catron, L. Newkirk, C. Taylor, Absolute Measurement of (n, 2n) Cross Sections at 14.1 Mev, Physical Review 111 (2) (1958) 616–621. doi:10.1103/PhysRev.111.616.

[3] N. Alpy, A. Terlain, V. Lorentz, Hydrogen extraction from Pb-17li: results with a 800 mm high packed column, Fusion Engineering and Design 49–50 (2000) 775–780. doi:10.1016/S0920-3796(00)00461-0.

[4] P. W. Humrickhouse, B. J. Merrill, Vacuum Permeator Analysis for Extraction of Tritium from DCLL Blankets, Fusion Science and Technology 68 (2) (2015) 295–302. doi:10.13182/FST14-941.

[5] H. Gräbner, H. Feuerstein, J. Oschinski, Compatibility of metals and alloys in liquid Pb-17li at temperatures up to 650C, Journal of Nuclear Materials 155157, Part 2 (1988) 702–704. doi:10.1016/0022-3115(88)90399-6.

[6] F. Okino, K. Noborio, R. Kasada, S. Konishi, Enhanced Mass Transfer of Deuterium Extracted from Falling Liquid Pb-17Li Droplets, Fusion Science and Technology 64 (3) (2013) 543 – 548. doi:10.13182/FST12-546.

[7] G. Pierini, F. Massetti, C. Rizzello, Feasibility study of tritium recovery systems from 83Pb17Li breeding material of a D-T fusion reactor, Fusion Technology 1984 (1985) 463–471.

[8] Y. Yamamoto, M. Ichinose, F. Okino, K. Noborio, S. Konishi, Design of Tritium Collecting System from LiPb and LiPb Dropping Experiment, Fusion Science and Technology 60 (2) (2011) 558–562.

[9] F. Okino, K. Noborio, Y. Yamamoto, S. Konishi, Vacuum sieve tray for tritium extraction from liquid Pb-17li, Fusion Engineering and Design 87 (7-8) (2012) 1014–1018. doi:10.1016/j.fusengdes.2012.02.071.

[10] F. Okino, K. Noborio, R. Kasada, S. Konishi, Deuterium Transport Prediction in Oscillating Liquid Pb-17li Droplet, Fusion Science and Technology 64 (3) (2013) 549–551.

[11] J. Crank, The mathematics of diffusion, Clarendon Press, Oxford [Eng], 1975.

[12] F. Reiter, Solubility and diffusivity of hydrogen isotopes in liquid Pb-17li, Fusion Engineering and Design 14 (3-4) (1991) 207–211. doi:10.1016/0920-3796(91)90003-9.

[13] C. Colebrook, Turbulent flow in pipes, with particular reference to the transition region between smooth and rough pipe laws, Journal of the Institution of Civil Engineers 11 (1939) 133–156. doi:10.1680/ijoti.1939.13150.

[14] T. Serghides, Estimate friction factor accurately, Chemical Engineering 91 (5) (1984) 63–64.

[15] D. J. Zigrang, N. D. Sylvester, A Review of Explicit Friction Factor Equations, Journal of Energy Resources Technology 107 (2) (1985) 280–283. doi:10.1115/1.3231190.

[16] S. Zinkle, Summary of Physical Properties for Lithium, Pb-17li, and $(LiF)_nBeF_2$ Coolants, APEX Study Meeting, Sandia National Lab (1998).

[17] S. V. Stankus, R. A. Khairulin, A. G. Mozgovoy, V. V. Roshchupkin, M. A. Pokrasin, The density and thermal expansion of eutectic alloys of lead with bismuth and lithium in condensed state, Journal of Physics: Conference Series 98 (6). doi:10.1088/1742-6596/98/6/062017.

[18] A. Aiello, A. Ciampichetti, G. Benamati, Determination of hydrogen solubility in lead lithium using sole device, Fusion Engineering and Design 81 (1-7) (2006) 639–644. doi:10.1016/j.fusengdes.2005.06.364.

[19] Y. Edao, H. Noguchi, S. Fukada, Experiments of hydrogen isotope permeation, diffusion and dissolution in Li-Pb, Journal of Nuclear Materials 417 (1-3) (2011) 723–726. doi:10.1016/j.jnucmat.2010.12.126.

[20] Y. Chan, E. Veleckis, A thermodynamic investigation of dilute solutions of hydrogen in liquid Li-Pb alloys, Journal of Nuclear Materials 123 (1-3) (1984) 935–940. doi:10.1016/0022-3115(84)90198-3.

[21] H. Katsuta, H. Iwamoto, H. Ohno, Hydrogen solubility in liquid Li17Pb83, Journal of Nuclear Materials 133-134 (1985) 167–170.

doi:10.1016/0022-3115(85)90127-8.
[22] Swagelok Catalogue: Bellow-Sealed Valves (Apr. 2014).
[23] R. Mulley, Flow of Industrial Fluids: Theory and Equations, CRC Press, 2004.
[24] M. Utili, M. Oron-Carl, Preliminary PFD of WCLL/HCLL LiPb loops, systems design and analyses, Tech. Rep. WPBB-DEL-D-511-01a, ENEA (Feb. 2015).
[25] M. Utili, M. Oron-Carl, Preliminary PFD of DCLL LiPb loop, system design and analyses, Tech. Rep. WPBB-DEL-D-511-02a, ENEA (Feb. 2015).
[26] R. Longhurst, R. Dolan, HYLIFE-II Tritium Management System, EGG-FSP-9971.
[27] F. Okino, P. Calderoni, R. Kasada, S. Konishi, Feasibility analysis of vacuum sieve tray for tritium extraction in the HCLL test blanket system, Fusion Engineering and Design-doi:10.1016/j.fusengdes.2015.10.004.
[28] K. Ioki, W. Dnner, K. Koizumi, V. A. Krylov, A. Cardella, F. Elio, M. Onozuka, I. J. C. Team, I. H. Teams, ITER-FEAT vacuum vessel and blanket design features and implications for the R&D programme, Nuclear Fusion 41 (3) (2001) 265. doi:10.1088/0029-5515/41/3/303.